Available online at www.sciencedirect.com
SCIENCE DIRECT®
International Journal of Heat and Mass Transfer 47 (2004) 5741–5747
International Journal of HEAT and MASS TRANSFER
www.elsevier.com/locate/ijhmt

End effects of heat conduction in circular cylinders of functionally graded materials and laminated composites

Jiann-Quo Tarn *, Yung-Ming Wang

Department of Civil Engineering, National Cheng Kung University, Tainan 70101, Taiwan, ROC

Received 1 August 2003; received in revised form 15 June 2004
Available online 7 October 2004

Abstract

Heat conduction in circular cylinders of functionally graded materials and laminated composites is studied with emphasis on the end effects. By means of matrix algebra and eigenfunction expansion, the decay length that characterizes the end effects on the thermal filed is evaluated and the 2D solution as a useful approximation assessed.

1. Introduction

When a cylindrical prismatic body is subjected to thermal loads that do not vary axially, the problem of heat conduction may be formulated as 2D provided that the temperature and heat flux over the end surfaces are specified in the same way as those in every other cross section of the body. For the 2D solution to be exact the end conditions cannot be prescribed arbitrarily, otherwise the thermal field will be disturbed by the end conditions. Questions arises as to under what circumstances can the 2D solution be used as an approximation. The purpose of this work is to evaluate the significance of the end effects through an exact analysis of heat conduction in circular cylinders of functionally graded materials (FGM) and laminated composites subjected to 2D thermal loads and arbitrary end conditions.

Solutions of heat conduction have been obtained, by and large, for homogeneous media with isotropy or special anisotropy [1–4]. For problems of a multilayered system a conventional approach is to express the field equations in terms of temperature and solve the governing equation for each layer, and then impose the interfacial continuity and boundary conditions (BC) to obtain the solution. Following this layerwise approach, one has to deal with the unpleasant task of determining the eigensolution of a $2m \times 2m$ matrix, m being the number of layers. In case the body is anisotropic and inhomogeneous, the difficulty in solving the governing equation has to be overcome to begin with. Herein we present a state space approach [5,6] for radially inhomogeneous, cylindrically anisotropic circular cylinders. Based on the approach, the eigensolution for a laminated system is determined by simple manipulation of 2×2 matrices, regardless of the number of layers.

It is known that the solution for a finite cylinder subjected to 2D thermal loads with prescribed end conditions may be determined by superposing the solutions for two fundamental problems: the first one is a 2D problem of an infinitely long cylinder subjected to the prescribed 2D thermal loads; the second one is a 3D problem of the cylinder subjected to homogeneous BC and arbitrary end conditions. For the purpose of evaluating the end effects it suffices to consider the second fundamental problem

* Corresponding author. Fax: +886 6 2358542.
E-mail address: jqtarn@mail.ncku.edu.tw (J.-Q. Tarn).

0017-9310/$ - see front matter
doi:10.1016/j.ijheatmasstransfer.2004.08.003

since the first fundamental solution [7] is independent of z. As a benchmark, an exact solution for the problem with a power-law radial inhomogeneity is derived as well, which enables us to assess the 2D solution as a useful approximation for the problem.

2. State space formulation

Consider heat conduction in a circular cylinder subjected to 2D thermal loads and prescribed end conditions. Referred to cylindrical coordinates (r,θ,z), the medium is radially inhomogeneous and cylindrically anisotropic. The Fourier law of heat conduction [1] is

$$\begin{bmatrix} q_r \\ q_\theta \\ q_z \end{bmatrix} = -\begin{bmatrix} k_{rr} & k_{r\theta} & k_{zz} \\ k_{r\theta} & k_{\theta\theta} & k_{\theta z} \\ k_{rz} & k_{\theta z} & k_{zz} \end{bmatrix} \begin{bmatrix} T_{,r} \\ r^{-1}T_{,\theta} \\ T_{,z} \end{bmatrix}, \tag{1}$$

where the comma denotes partial differentiation with respect the suffix variables; q_r,q_θ,q_z are the heat flux in the r, θ, z directions; T denotes the temperature; $k_{ij} = k_{ij}(r)$ (i, $j = r$,θ,z) are the conductivity coefficients for the radially inhomogeneous medium.

The heat balance equation for steady-state heat conduction without source or sink is

$$\frac{1}{r}\frac{\partial(rq_r)}{\partial r} + \frac{1}{r}\frac{\partial q_\theta}{\partial \theta} + \frac{\partial q_z}{\partial z} = 0. \tag{2}$$

In the state space approach, we choose $[T\, rq_r]$ to be the state vector and express Eqs. (1) and (2) into a state equation and an output equation. To this end, first we express $T_{,r}$ in terms of the state vector using Eq. $(1)_1$ to obtain

$$r\frac{\partial T}{\partial r} = -k_{rr}^{-1}\begin{bmatrix} k_{r\theta}\partial_\theta + k_{rz}r\partial_z & 1 \end{bmatrix} \begin{bmatrix} T \\ rq_r \end{bmatrix}, \tag{3}$$

where ∂_θ and ∂_z denote the partial derivatives with respect to θ and z, respectively.

Substituting Eq. (3) in Eqs. $(1)_2$ and $(1)_3$ yields

$$\begin{bmatrix} rq_\theta \\ rq_z \end{bmatrix} = k_{rr}^{-1}\begin{bmatrix} \tilde{k}_{\theta\theta}\partial_\theta + \tilde{k}_{\theta z}r\partial_z & k_{r\theta} \\ \tilde{k}_{\theta z}\partial_\theta + \tilde{k}_{zz}r\partial_z & k_{rz} \end{bmatrix} \begin{bmatrix} T \\ rq_r \end{bmatrix}, \tag{4}$$

where

$$\tilde{k}_{ij} = k_{ri}k_{rj} - k_{rr}k_{ij}.$$

Substituting Eq. (4) into Eq. (2) and casting the resulting equation and Eq. $(1)_1$ into a matrix differential equation, we obtain

$$r\frac{\partial}{\partial r}\begin{bmatrix} T \\ rq_r \end{bmatrix} = -k_{11}^{-1}\begin{bmatrix} k_{r\theta}\partial_\theta + k_{rz}r\partial_z & 1 \\ \tilde{k}_{\theta\theta}\partial_{\theta\theta} + 2\tilde{k}_{\theta z}r\partial_{\theta z} + \tilde{k}_{zz}r^2\partial_{zz} & k_{r\theta}\partial_\theta + k_{rz}r\partial_z \end{bmatrix} \times \begin{bmatrix} T \\ rq_r \end{bmatrix}. \tag{5}$$

Eq. (5) is the state equation for the problem. Once it is solved together with appropriate BC, q_θ and q_z follow from the output equation, Eq. (4). Three types of BC are considered: (1) prescribed surface temperature, (2) prescribed heat flux across the surface, (3) linear heat transfer on the cylindrical surfaces and on the ends. These BC can be expressed in the form

$$\left(\begin{bmatrix} h_1 & h_2r^{-1} \end{bmatrix}\begin{bmatrix} T \\ rq_r \end{bmatrix}\right)_{r=a} = F_a(\theta),$$
$$\left(\begin{bmatrix} h_3 & h_4r^{-1} \end{bmatrix}\begin{bmatrix} T \\ rq_r \end{bmatrix}\right)_{r=b} = F_b(\theta), \tag{6}$$

$$\left(\begin{bmatrix} \tilde{h}_1 & \tilde{h}_2r^{-1} \end{bmatrix}\begin{bmatrix} T \\ rq_z \end{bmatrix}\right)_{z=0} = G_0(r,\theta),$$
$$\left(\begin{bmatrix} \tilde{h}_3 & \tilde{h}_4r^{-1} \end{bmatrix}\begin{bmatrix} T \\ rq_z \end{bmatrix}\right)_{z=l} = G_l(r,\theta), \tag{7}$$

where $G_0(r,\theta)$ and $G_l(r,\theta)$ are prescribed functions on the end surfaces $z = 0$ and l; h_i and $\tilde{h}_i$ are given parameters to designate various BC; $F_a(\theta)$ and $F_b(\theta)$ are the 2D thermal loads on $r = a$ and b. To evaluate the end effects it suffices to consider $F_a(\theta) = F_b(\theta) = 0$. For a solid cylinder the BC on $r = a$ is replaced by requiring the temperature be bounded at $r = 0$.

For a multilayered cylinder composed of m layers, the conditions of interfacial continuity require

$$\begin{bmatrix} T & rq_r \end{bmatrix}_{k+1} = \begin{bmatrix} T & rq_r \end{bmatrix}_k \quad \text{on } r = r_k \tag{8}$$

where r_k denotes the outer radius of the k-th coaxial layer, $k = 1,2, \ldots, m-1$.

3. Piecewise-constant approximation

We seek the solution to Eq. (5) in the form

$$\begin{bmatrix} T \\ rq_r \end{bmatrix} = \sum_{n=-\infty}^{\infty}\begin{bmatrix} T_n(r) \\ rq_{rn}(r) \end{bmatrix} e^{-\alpha_n z/b}e^{in\theta} + \sum_{n=-\infty}^{\infty}\begin{bmatrix} \tilde{T}_n(r) \\ r\tilde{q}_{rn}(r) \end{bmatrix} e^{\beta_n(z-l)/b}e^{in\theta}, \tag{9}$$

where $T_n(r)$ and $q_{rn}(r)$ are unknown functions of r, α_n and β_n are dimensionless parameters to be determined. It can be shown that α_n and β_n are eigenvalues of the problem and they are *real*. Thus, for positive α_n, as z increases, the influence of the first series decreases and that of the second series increases, so that the largest positive value of α_n dictates the decay from $z = 0$ and the largest positive value of β_n dictates the decay from $z = l$. For a semi-infinite cylinder, $l \to \infty$, the second series disappears.

Substitution of Eq. (9) in Eq. (5) yields two sets of equations:

$$\frac{\mathrm{d}}{\mathrm{d}\rho}\mathbf{X}_n(\rho) = \mathbf{H}_n(\rho)\mathbf{X}_n(\rho),$$
$$\frac{\mathrm{d}}{\mathrm{d}\rho}\widetilde{\mathbf{X}}_n(\rho) = \widetilde{\mathbf{H}}_n(\rho)\widetilde{\mathbf{X}}_n(\rho), \tag{10}$$

where $c \leqslant \rho \leqslant 1$, $\rho = r/b$, $c = a/b$, and

$$\mathbf{H}_n(\rho) = \mathbf{A}_n + \alpha_n\rho\mathbf{B}_n + \alpha_n^2\rho^2\mathbf{C},$$
$$\widetilde{\mathbf{H}}_n(\rho) = \mathbf{A}_n - \beta_n\rho\mathbf{B}_n + \beta_n^2\rho^2\mathbf{C},$$
$$\mathbf{X}_n(\rho) = \begin{bmatrix} T_n(\rho) \\ \rho q_{rn}(\rho) \end{bmatrix}, \quad \widetilde{\mathbf{X}}_n(\rho) = \begin{bmatrix} \widetilde{T}_n(\rho) \\ \rho\tilde{q}_{rn}(\rho) \end{bmatrix},$$
$$\mathbf{A}_n = \rho^{-1}k_{11}^{-1}\begin{bmatrix} -ink_{r\theta} & -b \\ n^2\tilde{k}_{\theta\theta}b^{-1} & -ink_{r\theta} \end{bmatrix},$$

$$\begin{vmatrix} h_1\Gamma_{11}(c,\alpha_n) + h_2c^{-1}\Gamma_{21}(c,\alpha_n) & h_1\Gamma_{12}(c,\alpha_n) + h_2c^{-1}\Gamma_{22}(c,\alpha_n) \\ h_3 & h_4 \end{vmatrix} = 0, \tag{14}$$

$$\mathbf{B}_n = \rho^{-1}k_{11}^{-1}\begin{bmatrix} k_{rz} & 0 \\ 2in\tilde{k}_{\theta z}b^{-1} & k_{13} \end{bmatrix},$$
$$\mathbf{C} = \rho^{-1}k_{11}^{-1}\begin{bmatrix} 0 & 0 \\ -\tilde{k}_{zz}b^{-1} & 0 \end{bmatrix}.$$

A formal solution to Eq. (10) may be written in Peano expansion [8], however, it is virtually impossible to determine the transfer matrix from the expansion since it is not a closed form and the system matrix $\mathbf{H}_n(\rho)$ contains unknown parameters. We now present a useful scheme based on piecewise-constant approximation of an arbitrary radial inhomogeneity. The continuity at the jumps introduced by the approximation is satisfied by using the transfer matrix. The scheme amounts to approximating a radially inhomogeneous cylinder by a multilayered cylinder composed of homogeneous coaxial layers.

For each homogeneous layer an explicit solution of Eq. (10) is obtained by setting $\mu = 0$ in Eqs. (17)–(20) in Section 4. At this stage we may express the solution for the nth harmonics by

$$\mathbf{X}_k(\rho) = \mathbf{P}_k(\rho,\rho_k)\mathbf{X}_k(\rho_k), \quad \rho_{k+1} \leqslant \rho \leqslant \rho_k \tag{11}$$

where k runs from 1 to m, m being the number of the coaxial layers; ρ_{k+1} and ρ_k denote the inner and outer radii of the k-th layer. Thus, $k = 1$ denotes the outer layer with $\rho_1 = 1$, $k = m$ denotes the inner layer with $\rho_{m+1} = c$.

The interfacial continuity conditions at $\rho = \rho_{k+1}$ are satisfied by letting

$$\mathbf{X}_{k+1}(\rho_{k+1}) = \mathbf{X}_k(\rho_{k+1}). \tag{12}$$

Using Eqs. (11) and (12) recursively from the outer layer inward, we arrive at

$$\mathbf{X}_k(\rho) = \mathbf{\Gamma}_k(\rho,\alpha_n)\mathbf{X}_1(1), \tag{13}$$

where

$$\mathbf{\Gamma}_k(\rho,\alpha_n) = \begin{bmatrix} \Gamma_{11}(\rho,\alpha_n) & \Gamma_{12}(\rho,\alpha_n) \\ \Gamma_{21}(\rho,\alpha_n) & \Gamma_{22}(\rho,\alpha_n) \end{bmatrix} = \begin{cases} \mathbf{P}_k(\rho,\rho_k), & k = 1; \\ \mathbf{P}_k(\rho,\rho_k)\mathbf{\Gamma}_{k-1}(\rho_k,\alpha_n), & k = 2,\ldots,m. \end{cases}$$

Setting $\rho = c$ in Eq. (13) and imposing on it the homogeneous BC at $\rho = c$ and 1 yields a system of homogeneous equations, to which a non-trivial solution exists if (14), from which the eigenvalues α_n and subsequently the associated eigenvectors can be determined.

There follows

$$\begin{bmatrix} T \\ \rho q_r \end{bmatrix} = \sum_{s=1}^{\infty}\sum_{n=-\infty}^{\infty}\begin{bmatrix} \Gamma_{11}(\rho,\alpha_n) & \Gamma_{12}(\rho,\alpha_n) \\ \Gamma_{21}(\rho,\alpha_n) & \Gamma_{22}(\rho,\alpha_n) \end{bmatrix}\begin{bmatrix} h_4 \\ -h_3 \end{bmatrix} \times \left[c_{ns}\mathrm{e}^{-|\alpha_{ns}|z/b} + d_{ns}\mathrm{e}^{|\alpha_{ns}|(z-l)/b}\right]\mathrm{e}^{in\theta}, \tag{15}$$

where the constants c_{ns} and d_{ns} are determined using the end conditions.

4. Exact solution for power-law inhomogeneity

An exact solution for the problem can be determined if the radial inhomogeneity is described by

$$k_{ij} = k_{ij}(r) = \kappa_{ij}(r/b)^{\mu}, \tag{16}$$

where κ_{ij} and μ are real constants. The radial inhomogeneity of a linear variation is given by setting $\mu = 1$; a homogeneous material by setting $\mu = 0$.

The solution for the first fundamental problem has been given elsewhere [7]. Here we are concerned with the solution for the second fundamental problem. With Eq. (16), we can express ρq_{rn} in terms of T_n by using the first equation of Eq. $(10)_1$ and substitute it into the second equation of Eq. $(10)_1$ to obtain

$$\rho^2\frac{\mathrm{d}^2T_n}{\mathrm{d}\rho^2} + \left(1 + \mu + 2in\frac{\kappa_{r\theta}}{\kappa_{rr}}\right)\rho\frac{\mathrm{d}T_n}{\mathrm{d}\rho} + \left(\frac{\kappa_{zz}}{\kappa_{rr}}\alpha_n^2\rho^2 + in\mu\frac{\kappa_{r\theta}}{\kappa_{rr}} - n^2\frac{\kappa_{\theta\theta}}{\kappa_{rr}}\right)T_n = 0. \tag{17}$$

The solution of Eq. (17) is

$$T_n(\rho) = \rho^{-\eta}[c_{1n}J_p(\lambda_n\rho) + c_{2n}Y_p(\lambda_n\rho)], \tag{18}$$

where $J_p(x)$, $Y_p(x)$ are Bessel functions of the first and second kind of the p-th order, p is real for a real μ; c_{1n} and c_{2n} are constants of linear combination; and

$$\eta = \frac{\mu}{2} + in\frac{\kappa_{r\theta}}{\kappa_{rr}}, \quad \lambda_n = \left(\frac{\kappa_{zz}}{\kappa_{rr}}\right)^{1/2}\alpha_n,$$

$$p = \left[\left(\frac{\mu}{2}\right)^2 + n^2\left[\frac{\kappa_{\theta\theta}}{\kappa_{rr}} - \left(\frac{\kappa_{r\theta}}{\kappa_{rr}}\right)^2\right]\right]^{1/2}.$$

There follows

$$\begin{bmatrix} T_n(\rho) \\ \rho q_{rn}(\rho) \end{bmatrix} = \rho^{-\eta}\begin{bmatrix} J_p(\lambda_n\rho) & Y_p(\lambda_n\rho) \\ G_1(\lambda_n\rho) & G_2(\lambda_n\rho) \end{bmatrix}\begin{bmatrix} c_{1n} \\ c_{2n} \end{bmatrix}, \tag{19}$$

where

$$G_1(\lambda_n\rho) = \kappa_{rr}\rho^{\mu}[\lambda_n\rho J_{p+1}(\lambda_n\rho) + (\mu/2 - p)J_p(\lambda_n\rho)],$$

$$G_2(\lambda_n\rho) = \kappa_{rr}\rho^{\mu}[\lambda_n\rho Y_{p+1}(\lambda_n\rho) + (\mu/2 - p)Y_p(\lambda_n\rho)].$$

Expressing c_{1n} and c_{2n} in terms of $T_n(1)$ and $q_{rn}(1)$ and substituting it back into Eqs. (19), we obtain

$$\begin{bmatrix} T_n(\rho) \\ \rho q_{rn}(\rho) \end{bmatrix} = \begin{bmatrix} Q_{11}(\rho,\lambda_n) & Q_{12}(\rho,\lambda_n) \\ Q_{21}(\rho,\lambda_n) & Q_{22}(\rho,\lambda_n) \end{bmatrix}\begin{bmatrix} T_n(1) \\ q_{rn}(1) \end{bmatrix}, \quad c \leqslant \rho \leqslant 1 \tag{20}$$

which is the counterpart of Eq. (13), where

$$Q_{11}(\rho,\lambda_n) = \rho^{-\eta}[\lambda_n F(\rho,1,p,p+1) + (\mu/2-p)F(\rho,1,p,p)]/\Delta,$$

$$Q_{12}(\rho,\lambda_n) = b\kappa_{rr}^{-1}\rho^{-\eta}F(1,\rho,p,p)/\Delta,$$

$$Q_{21}(\rho,\lambda_n) = b^{-1}\kappa_{rr}\rho^{\mu-\eta}\{\lambda_n^2\rho F_n(\rho,1,p+1,p+1) + (\mu/2-p)^2F(\rho,1,p,p) + \lambda_n(\mu/2-p) \times [\rho F(\rho,1,p+1,p) + F(\rho,1,p,p+1)]\}/\Delta,$$

$$Q_{22}(\rho,\lambda_n) = \rho^{\mu-\eta}[\lambda_n\rho F(1,\rho,p,p+1) + (\mu/2-p)F(1,\rho,p,p)]/\Delta,$$

$$F(x,y,p,q) = J_p(\lambda_n x)Y_q(\lambda_n y) - J_q(\lambda_n y)Y_p(\lambda_n x),$$
$$\Delta = \lambda_n F(1,1,p,p+1,\lambda_n).$$

Imposing on Eq. (20) the homogeneous BC on $\rho = c$ and 1 yields a system of homogeneous equations, to which a non-trivial solution exists if

$$\begin{vmatrix} h_1Q_{11}(c,\lambda_n) + h_2c^{-1}Q_{21}(c,\lambda_n) & h_1Q_{12}(c,\lambda_n) + h_2c^{-1}Q_{22}(c,\lambda_n) \\ h_3 & h_4 \end{vmatrix} = 0 \tag{21}$$

from which the eigenvalues λ_n and the associated eigenvectors can be determined.

For a solid cylinder the terms of $Y_p(\rho)$ in Eq. (18) must be dropped so that the temperature at the axis $r = 0$ is bounded. As a result,

$$\begin{bmatrix} T_n(\rho) \\ \rho q_{rn}(\rho) \end{bmatrix} = \begin{bmatrix} \widetilde{Q}_{11}(\rho,\lambda_n) & 0 \\ 0 & \widetilde{Q}_{22}(\rho,\alpha_n) \end{bmatrix}\begin{bmatrix} T_n(1) \\ q_{rn}(1) \end{bmatrix}, \quad 0 < \rho \leqslant 1 \tag{22}$$

where

$$\widetilde{Q}_{11}(\rho,\lambda_n) = \rho^{-\eta}\frac{J_p(\lambda_n\rho)}{J_p(\lambda_n)},$$

$$\widetilde{Q}_{22}(\rho,\lambda_n) = \rho^{\mu-\eta}\frac{\lambda_n\rho J_{p+1}(\lambda_n\rho) + (\mu/2-p)J_p(\lambda_n\rho)}{\lambda_n J_{p+1}(\lambda_n) + (\mu/2-p)J_p(\lambda_n)}.$$

5. Characteristic decay length

A simple measure of the end effects is the characteristic decay length which is the distance that marks the region from the ends where the thermal field is no longer significantly affected by the end conditions. According to Eq. (9), we may define the characteristic decay length as

$$L = b\frac{\ln 100}{\alpha_{ns}}, \tag{23}$$

which is the distance measured from the end beyond which the temperature and heat flux reduce to 1% of their values on the end.

To assess the end effects, we have computed the characteristic decay length for a thin-walled tube ($a/b = 0.9$) and thick-walled cylinders ($a/b = 0.1; 0.5$) under various BC. The radial inhomogeneity is assumed to follow the power law in order to validate the numerical results. Various material parameters were taken. The BC considered are either temperature-prescribed (T) or flux-prescribed (F) on $r = a$ and b. For brevity, we use the notation T–T for the temperature-prescribed BC on $r = a$ and b; T–F for temperature-prescribed on $r = a$ and flux-prescribed on $r = b$, and so forth.

The accuracy based on the piecewise-constant approximation depends on the number of the fictitious layers taken to approximate the radial inhomogeneity. It was found that the results are accurate to 10^{-3} compared with the exact solution by taking less than 20 fictitious layers. In the case of a thin-walled cylinder it is sufficient to take 5 layers to obtain accurate results. Even modeling the radial inhomogeneity of a thick-walled cylinder by taking as many as 100 layers, it took only seconds in computation using a PC.

Another useful check is to consider a thin-walled homogeneous tube. With $c = a/b \to 1$, $\mu = 0$, and $n = 0$

(symmetric mode), Eq. (17) under the homogeneous BC can be solved to obtain

$$\alpha_{0m} = \frac{1}{b}\left[\frac{m^2\pi^2}{(1-c)^2}+\frac{1}{4}\right]^{1/2}\left(\frac{\kappa_{rr}}{\kappa_{zz}}\right)^{1/2}$$
$$\approx \frac{m\pi}{b(1-c)}\left(\frac{\kappa_{rr}}{\kappa_{zz}}\right)^{1/2}, \quad (c \neq 1) \tag{24}$$

The first few eigenvalues of the hollow cylinder for various a/b and μ are given in Tables 1 and 2. The numerical results for $\mu = 0$, $a/b = 0.9$ agree well with those obtained according to Eq. (24). The value of μ has little influence on a thin-walled tube. This is expected because the radial inhomogeneity through a short thickness of a thin-walled tube generally should not exhibit marked variation. The effects of radial inhomogeneity and cylindrical anisotropy are insignificant for

Table 1
The first 5 eigenvalues for hollow cylinders under temperature-prescribed (T–T) BC

a/b	μ	λ_{01}	λ_{02}	λ_{03}	λ_{04}	λ_{05}
0.1	0	3.3139	6.8576	10.3774	13.8864	17.3896
	0.5	3.3597	6.8889	10.4012	13.9055	17.4056
	1	3.4907	6.9813	10.4720	13.9626	17.4533
	2	3.9409	7.3306	10.7484	14.1886	17.6433
	5	5.7649	9.1067	12.3671	15.6263	18.9099
	10	8.7715	12.3386	15.7003	18.9806	22.2197
0.5	0	6.2461	12.5469	18.8364	25.1228	31.4080
	0.5	6.2554	12.5517	18.8397	25.1253	31.4100
	1	6.2832	12.5664	18.8496	25.1327	31.4159
	2	6.3932	12.6247	18.8889	25.1624	31.4397
	5	7.1116	13.0261	19.1625	25.3692	31.6058
	10	9.1900	14.3733	20.1128	26.0963	32.1928
0.9	0	31.4115	62.8296	94.2463	125.6626	157.0787
	0.5	31.4126	62.8302	94.2466	125.6629	157.0790
	1	31.4159	62.8318	94.2478	125.6637	157.0796
	2	31.4292	62.8385	94.2522	125.6670	157.0823
	5	31.5217	62.8849	94.2831	125.6902	157.1009
	10	31.8499	63.0502	94.3935	125.7731	157.1671

Table 2
The first 6 eigenvalues for hollow cylinders under flux-prescribed (F–F) BC

a/b	μ	λ_{00}	λ_{01}	λ_{02}	λ_{03}	λ_{04}	λ_{05}
0.1	0	0	3.9409	7.3306	10.7484	14.1886	17.6433
	0.5	0	4.2226	7.5723	10.9482	14.3553	17.7847
	1	0	4.5223	7.8466	11.1835	14.5553	17.9561
	2	0	5.1423	8.4574	11.7385	15.0441	18.3834
	5	0	6.9880	10.4179	13.7024	16.9396	20.1652
	10	0	9.9361	13.5893	17.0038	20.3208	23.5863
0.5	0	0	6.3931	12.6247	18.8889	25.1624	31.4397
	0.5	0	6.4743	12.6683	18.9184	25.1846	31.4575
	1	0	6.5720	12.7214	18.9544	25.2118	31.4793
	2	0	6.8138	12.8555	19.0457	25.2808	31.5347
	5	0	7.8450	13.4711	19.4711	25.6038	31.7946
	10	0	10.1889	15.1100	20.6522	26.5148	32.5330
0.9	0	0	31.4292	62.8385	94.2522	125.6670	157.0823
	0.5	0	31.4391	62.8434	94.2555	125.6695	157.0843
	1	0	31.4512	62.8495	94.2596	125.6726	157.0867
	2	0	31.4821	62.8650	94.2699	125.6803	157.0928
	5	0	31.6271	62.9378	94.3185	125.7167	157.1221
	10	0	32.0408	63.1470	94.4582	125.8216	157.2060

the higher modes for a moderately thick cylinder ($a/b = 0.5$) and a thin-walled cylinder ($a/b = 0.9$). It can be shown that $\alpha_0 = 0$ is an eigenvalue under the *F–F* BC and the associated eigenvector is composed of a uniform temperature and a linearly distributed temperature in z. Indeed we found in Table 2 that the smallest eigenvalue is zero and the characteristic decay length is infinite. This indicates that the end effects are far-reaching; it affects the thermal field over the entire cylinder. Thus, when the heat flux is specified on the inner and outer surfaces, the thermal field must be determined through a 3D analysis.

The values of λ_{ns} under the *T–T* BC is given in Table 3, in which the values are less than 0.8, except for the

Table 3
Characteristic decay length $(L/b)(k_{rr}/k_{zz})^{1/2}$ for hollow cylinders under temperature-prescribed (*T–T*) BC

a/b	$\mu = 0$	0.5	1.0	2.0	5.0	10.0
0.1	1.3897	1.3707	1.3193	1.1686	0.7988	0.5250
0.5	0.7373	0.7362	0.7329	0.7203	0.6476	0.5011
0.9	0.1466	0.1466	0.1466	0.1465	0.1461	0.1446

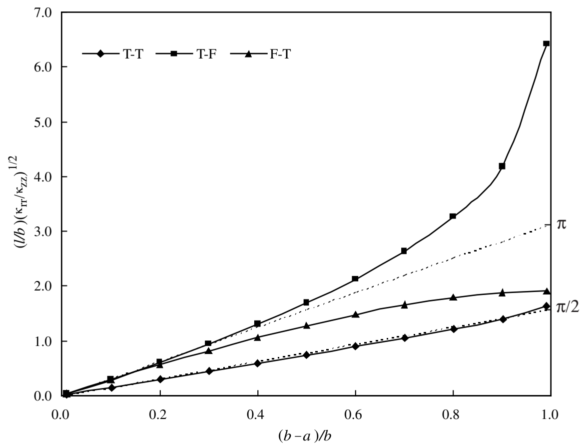

Fig. 1. Characteristic decay length with respect to the wall thickness of homogeneous hollow cylinders ($\mu = 0$) under various boundary conditions.

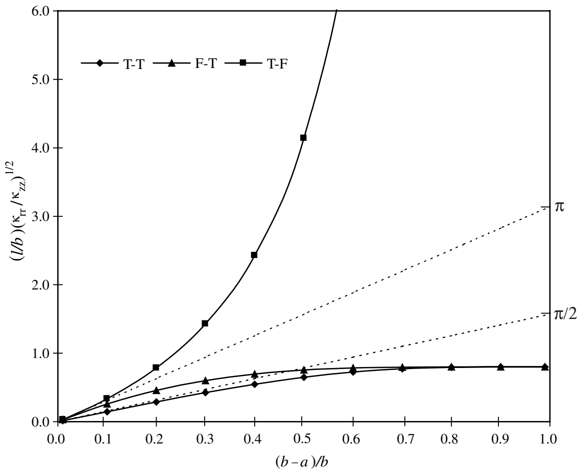

Fig. 2. Characteristic decay length with respect to the wall thickness of radially inhomogeneous hollow cylinders ($\mu = 5$) under various boundary conditions.

cylinder of a very large thickness ($a/b = 0.1$), thus the decay length for an isotropic hollow cylinder is less than b. With $k_{rr} = k_{\theta\theta} = 0.72\ W/(m \cdot K)$, $k_{zz} = 4.62\ W/(m \cdot K)$ for a typical unidirectional graphite/epoxy composite, the decay length is less than $2b$. In the case of a very thick graphite/epoxy composite cylinder ($a/b = 0.1$, $\mu = 0;0.5$) under the T–T BC, the decay length is about $3.5b$. In this case, the significance of the end effects depends on the length–diameter ratio of the cylinder.

Figs. 1 and 2 show the decay length with respect to the wall thickness of a homogeneous hollow cylinder ($\mu = 0$) and a radially inhomogeneous one ($\mu = 5$) under various BC. The decay length for the cylinder under the F–F BC is infinite and is not shown in the figure. In the case of the F–T BC, the decay length depends on the ratio of a/b. It could be as long as $15b$ for a homogeneous cylinder and tends to infinity for $\mu = 5$. In these cases a 3D analysis of the problem is necessary. The dashed lines in Figs. 1 and 2 are the lines according to the simplified formula for the thin-walled tube. Notably, the decay length of a hollow cylinder with a wall thickness $(b-a)/b < 0.2$ under the T–T BC is about half of those under the F–T and the T–F BC. This can be understood by considering a segment of a thin-walled tube. When the inner radius of the tube is large, the segment may be regarded as a thin plate. Under the homogeneous T–T BC, there should be no heat flux in the middle plane of the plate because of symmetry. Thus, a plate of thickness $2h$ under the homogeneous T–T BC may be viewed as a plate of thickness h under the homogeneous F–T BC or under the homogeneous T–F BC. When the thicknesses of the plate in three cases are the same, the decay length of the plate under the homogeneous T–T BC must be a half of those of the other two.

6. Conclusions

We have studied the end effects of heat conduction in a hollow or solid circular cylinder of FGM and laminated composites under 2D thermal loads and arbitrary end conditions. The significance of the end effects can be evaluated through a characteristic decay length. When the temperature is prescribed on the lateral surfaces, the end effects are confined to a local region near the ends and the 2D solution can be used to evaluate the thermal field in the region of a characteristic decay length from the ends. For other cases the end effects are far-reaching and the problem must be treated as 3D.

Acknowledgment

The work is supported by the National Science Council of Taiwan, ROC through grant NSC 92-2211-E006-070.

References

[1] M.N. Özisik, Heat Conduction, Wiley, New York, 1993.
[2] Y.P. Chang, C.H. Tsou, Heat conduction in an anisotropic medium homogeneous in cylindrical coordinates, steady state, J. Heat Transfer 99C (1977) 132–134.
[3] Y.P. Chang, C.H. Tsou, Heat conduction in an anisotropic medium homogeneous in cylindrical coordinates, unsteady state, J. Heat Transfer 99C (1977) 41–47.
[4] M.N. Özisik, S.M. Shouman, Transient heat conduction in an anisotropic medium in cylindrical coordinates, J. Franklin Inst. 309 (1980) 457–472.
[5] J.Q. Tarn, Exact solutions for functionally graded anisotropic cylinders subjected to thermal and mechanical loads, Int. J. Solids Struct. 38 (2001) 8189–8206.
[6] J.Q. Tarn, A state space formalism for anisotropic elasticity. Part II: cylindrical anisotropy, Int. J. Solids Struct. 39 (2002) 5157–5172.
[7] J.Q. Tarn, Y.M. Wang, Heat conduction in a cylindrically anisotropic tube of a functionally graded material, Chin. J. Mech. 19 (2003) 365–372.
[8] M.C. Pease, Methods of Matrix Algebra, Academic Press, New York, 1965.